communications biology

A Nature Portfolio journal

Article

https://doi.org/10.1038/s42003-025-08014-x

GRASPs link Reelin to the Golgi during neocortical development to control neuronal migration and dendritogenesis

Elisa Calvo-Jiménez, Kirsten Stam, Angélique Jossi & Yves Jossin

Reelin serves as a crucial regulator of brain organogenesis, playing a significant role in neuronal positioning and dendritogenesis. At subcellular level, it influences the translocation and remodeling of the Golgi apparatus. Despite its importance, the mechanisms by which Reelin governs the Golgi during neuronal migration and dendrite formation remain largely unknown. This study reveals that Reelin promotes de novo translation of Golgi Re-Assembly Stacking Proteins (GRASPs), which are essential for the functions of Reelin on cortical neurons. Downregulation of GRASPs in migrating excitatory neurons of the embryonic neocortex leads to disoriented cells during the multipolar phase of migration and an aberrant leading process length during locomotion. Postnatally, it results in mislocalized neurons displaying a disorganized Golgi structure and an improperly oriented, underdeveloped apical dendrite. Our findings position GRASPs and their role in Golgi morphology modulation as novel contributors to the Reelin-mediated processes during embryonic development of the mammalian neocortex.

The development of the cerebral cortex depends on the correct migration of its neurons from their birthplace to their final destination where they mature. Excitatory pyramidal neurons originate at the ventricular zone (VZ) and migrate through the cerebral wall in a dynamic manner. They transition from locomoting and unidirectional cells to a multipolar/multidirectional migration, then back to locomoting cells, ultimately reaching the top of the cortical plate (CP) where they finalize their migration with a terminal somal translocation[1–4]. The axon is established during the multipolar stage, while dendritic development occurs after completion of migration[5]. Pyramidal neurons have a single apical dendrite that extends towards the pia featuring apical secondary branches that terminate in layer I[6]. Additionally, several shorter basolateral dendrites emanate from the cell body and receive distinct synaptic outputs.

The Golgi apparatus is instrumental in cell polarization by directing lipids and proteins to specific subcellular localizations, thereby influencing the orientation of migration of various cell types, including neurons[1,7]. Indeed, the different steps of excitatory neurons migration are accompanied by changes in the subcellular localization and deployment of the Golgi apparatus[8]. Furthermore, the position of the Golgi apparatus and the adjoined centrosome is determinant for axon specification during the multipolar stage, and later for the asymmetrical development of dendrites[9–11]. Finally, specialized Golgi outposts populate dendrites, promoting the elaboration of dendritic branches[12].

Defects in neocortical architecture resulting from impaired migration or dendritic development are associated with a wide variety of human conditions such as lissencephalies, neuronal heterotopias, intellectual disabilities, epilepsy, autism spectrum disorders and schizophrenia[13–16]. The molecular mechanisms that govern Golgi positioning and the potential links with critical aspects of brain development are yet incompletely understood.

The Reelin pathway is a key regulator of several neuronal polarity events occurring during neocortical development[14]. It ensures the proper orientation of pyramidal neurons towards the CP during multipolar migration[17,18], and is essential for the completion of terminal somal translocation[4,19]. Additionally, Reelin stimulates dendritogenesis after completion of neuronal migration[20–23]. Despite the growing evidence that places Reelin signaling as a key player in the dynamics of the Golgi apparatus during cortical development[23–26], the specific molecular mechanisms involved are still largely unknown. This study aims to explore the role of a family of Golgi structure regulators, the Golgi Re-Assembly Stacking Proteins (GRASPs), in these critical Reelin-dependent processes.

The GRASPs (GRASP55 and GRASP65) self-interact to form *trans*-oligomers that tether adjacent Golgi membranes into stacks and ribbons to regulate Golgi structural plasticity in mammalian cells (Reviewed in ref. 27). GRASP proteins are anchored to the Golgi membrane via a myristic acid present on a N-terminal glycine. GRASP65 is predominantly found in the *cis*-Golgi, while GRASP55 is more abundant in the medial- and *trans*-

Laboratory of Mammalian Development & Cell Biology, Institute of Neuroscience, Université Catholique de Louvain, Brussels, Belgium.
e-mail: yves.jossin@uclouvain.be

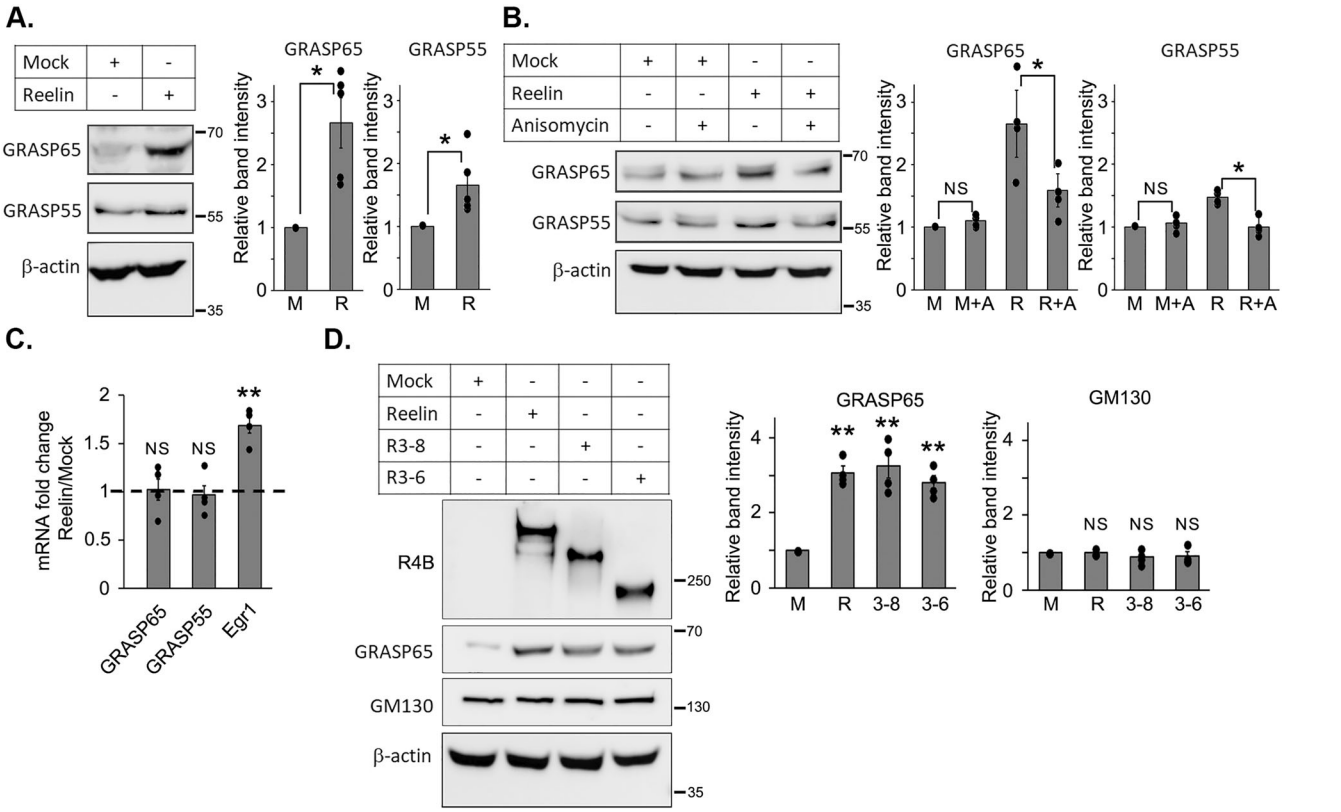

Fig. 1 | Reelin increases GRASPs protein levels via the stimulation of de novo translation. A, **B**, **D** Western blots or (**C**) RT-qPCR results of cell lysates from E16.5 mouse cortical neurons that were cultured for 4 days, followed by a 30-minute stimulation with Mock- and Reelin-conditioned media or small molecules inhibitors. The graphs in (**A**, **B**, **D**) show GRASPs or GM130 protein levels measured in Western Blot by densitometry with the Mock-stimulated condition set to 1 (mean ± s.e.m.). **A** Reelin treatment increases GRASP65 and GRASP55 protein levels ($n = 5$). **B** Inhibition of translation reduced the effect of Reelin on GRASP65 and GRASP55 protein level. Anisomycin was used at 40 μM for 45 min before and during Reelin treatment ($n = 4$). **C** The graph shows mRNA fold change after Reelin stimulation for *Grasp65*, *Grasp55*, and *Egr1* ($n = 4$). **D** Reelin full-length or its fragments R3-8 and R3-6 induced an increase in GRASP65 protein level but did not affect GM130 ($n = 4$). $^{**}p < 0.01$, $^{*}p < 0.05$, NS not significant.

cisternae. Depletion of a single GRASP in cultured cells leads to a decrease in the number of cisternae per Golgi stack, whereas double knockout (KO) of both GRASP proteins results in the dispersion the Golgi stack into single cisternae[28]. However, several other studies concluded that loss of GRASP proteins primarily impacts the formation of Golgi ribbons rather than the stacks themselves (Reviewed in ref. 29). The Golgi apparatus serves as a pivotal hub in the secretory pathway, and modifications of its structure influence protein trafficking, sorting and glycosylation. Research conducted in cell cultures has indicated that GRASPs are implicated in several physiological processes including cell cycle progression, cell adhesion, oriented cell migration, autophagy, and unconventional protein secretion (UPS)[30–35]. In accordance with their functions in UPS, GRASPs are also observed outside the Golgi structure in other subcellular location such as endosomes, autophagosomes and plasma membrane[34,36–38].

No overt developmental defects have been reported in the GRASP55 or 65 single KO mice[39,40]. However, while double KO for both GRASPs is embryonic lethal, a GRASP65 KO mouse crossed with a tamoxifen-induced GRASP55 conditional KO showed a reduced number of cisternae per Golgi stack and a compromised arrangement of Golgi ribbon in the small intestine cells that were examined. It is noteworthy that these mice still express a truncated GRASP55 which may account for the relatively mild phenotype observed[27,41]. Despite the critical role of the Golgi apparatus and the potential link between GRASP proteins and human brain malformations as well as cognitive impairment[42–44], the specific functions of GRASP55 and 65 in the developing neocortex remain unexplored.

Here, we show that Reelin induces an increase in GRASPs protein levels via de novo translation, the inhibition of which prevents Reelin-induced Golgi deployment and dendritic growth. In a manner akin to Reelin inhibition, GRASPs downregulation in the developing embryonic neocortex disrupts Golgi positioning during multipolar migration, and hinders proper cortical lamination. After completion of migration in the postnatal brain, the knockdown of GRASPs disrupts the polarized Golgi organization and interferes with dendrite morphogenesis of cortical excitatory neurons in vivo. Our findings elucidate a previously unknown function of GRASPs in shaping the developing cerebral cortex and provide insights into the regulatory effects of Reelin on the Golgi during these developmental processes.

Results

Reelin increases GRASPs protein levels via the stimulation of de novo translation

Previous research has indicated that Reelin and the LKB1/Stk25 signaling pathway have opposing influences on the control of Golgi morphology in hippocampal neurons through different unknown mechanisms[25]. Given that GRASPs are regulators of Golgi architecture and their role in the developing brain is unknown, we aimed to investigate their function in the Reelin signaling pathway. Upon stimulation of cultured primary cortical neurons with Reelin, we observed a significant increase in GRASP65 protein levels, while a comparatively smaller effect was detected for GRASP55 (Fig. 1A and Supplementary Fig. S1). Notably, the elevations in GRASP65 and 55 protein levels induced by Reelin were significantly attenuated by the pre-treatment with 40 μM anisomycin, a translation inhibitor, for 45 min prior to and during Reelin exposure, indicating that de novo translation is involved (Fig. 1B and Supplementary Fig. S1). Conversely, RT-qPCR analysis revealed that the mRNA levels of *GRASPs* remained unchanged by Reelin stimulation under our experimental conditions. As a control, the

known transcriptional target of Reelin, *Egr1*[45] exhibited an increase in expression (Fig. 1C).

Given the more pronounced effect of Reelin on GRASP65 compared to GRASP55, subsequent experiments were focused on GRASP65. We considered the possibility that the observed increase in protein levels might also result from degradation or processing mechanisms. However, our investigations revealed that the Reelin-induced increase in GRASP65 protein levels was not replicated by inhibitors targeting the proteasome, the lysosome, or Caspase3 (which is involved in GRASP cleavage[46]) (Supplementary Fig. S2).

Overall, these results demonstrate that the increase in GRASP protein levels in response to Reelin is primarily attributed to de novo translation, rather than being influenced by changes in mRNA levels or a reduction in protein degradation. While our data establish the effect of Reelin following a 30-minute stimulation, we also found that Reelin exerts a sustained influence, continuing to modulate GRASP65 protein levels in cortical neurons even after 15 h of exposure (Supplementary Fig S3).

Reelin undergoes processing by metalloproteinases, a crucial step that facilitates the diffusion of specific cleavage fragments into the intermediate zone (IZ) of the developing cortex, most likely trough the C-terminal cleavage between the Reelin repeated domains 6 and 7. This mechanism allows the N-terminal fragments, encompassing the N-terminus to the second or to the sixth Reelin repeated domains (respectively N-R2 and N-R6) and the central fragment, which includes the Reelin repeated domains 3 to 6 (R3-6), to reach multipolar migrating neurons located deeper within the tissue at the IZ[14,17,47,48]. Meanwhile, the full-length Reelin (and C-terminal fragments) remains in proximity to its source cells within the marginal zone (MZ).

Considering that R3-6 is the smallest active fragment of Reelin observed in vivo and is found in the CP and IZ, we tested whether this central fragment also influences GRASPs. Our findings indicate that both R3-6 and the larger fragment R3-8 are able to increase GRASP65 protein levels in cultured primary cortical neurons (Fig. 1D). However, there was no observed change in the protein levels of Golgi matrix protein 130 (GM130), another Golgi membrane protein involved in Golgi morphology[25,49] and known to interact with and stabilize GRASP65[50] (Fig. 1D).

In agreement with the hypothesis of an effect of Reelin and its fragments on GRASP65 protein level at the CP and IZ, we observed a stronger GRASP65 signal in the CP and IZ when compared to the signal at the ventricular /sub-subventricular zone (VZ/sVZ) in vivo (Supplementary Fig. S4).

These data suggest that Reelin regulates GRASP65 in cortical neuron located at the IZ and the CP.

Most of Reelin functions in the developing brain require the tyrosine phosphorylation of the intracellular adapter Disabled-1 (Dab1) by the Src family kinases (SFK) Src and Fyn[51–53]. To ascertain whether the impact of Reelin on GRASPs depends on this canonical Reelin signaling pathway, we either nucleofected primary cortical neurons for the expression of shRNAs targeting Dab1 or treated the neurons with the SFK inhibitor PP2. We found that the effect of Reelin on GRASP65 protein levels is inhibited by the

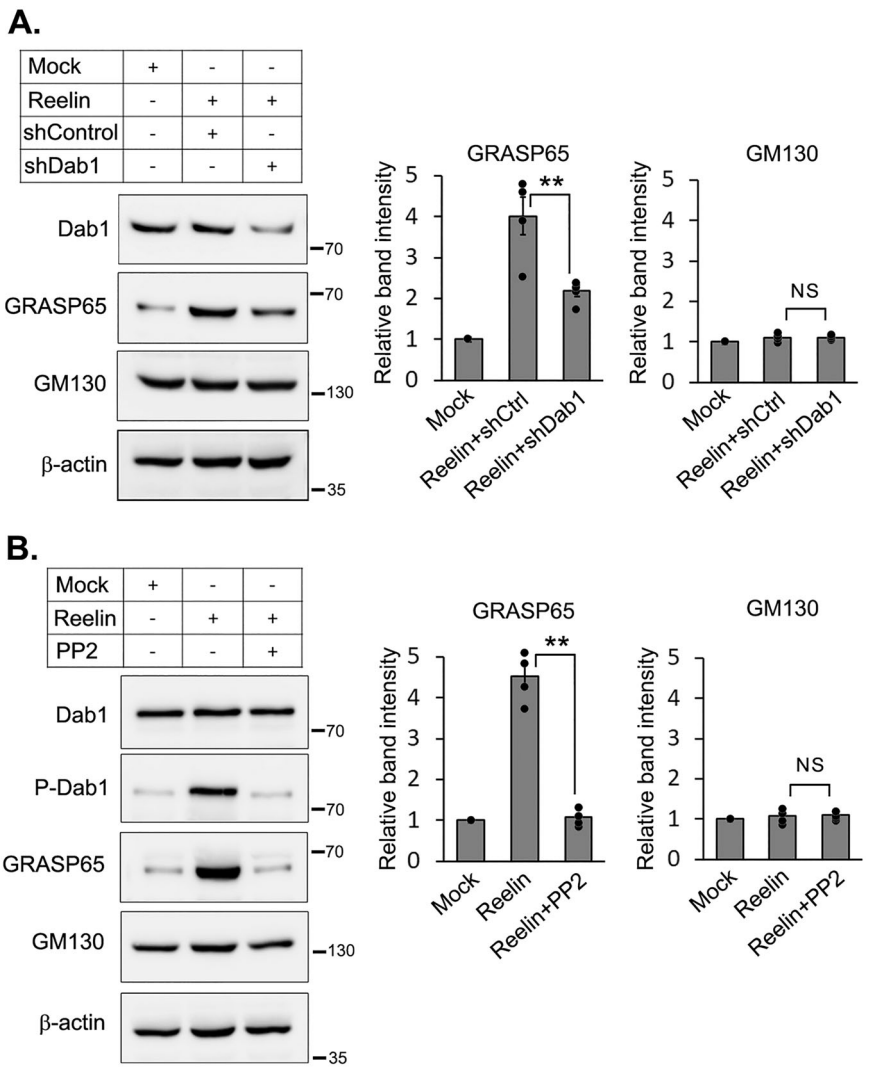

Fig. 2 | Reelin increases GRASPs protein levels through the canonical Dab1 pathway. Western blots of cell lysates from E16.5 mouse cortical neurons that were cultured for 4 days, followed by a 30-min stimulation with Mock- and Reelin-conditioned media. The graphs show GRASPs or GM130 protein levels measured in Western Blot by densitometry with the Mock-stimulated condition set to 1 (mean ± s.e.m.). **A** Neurons were nucleofected with an efficiency of about 60–70% for the expression of shRNAs against *Dab1* (shDab1) or a control shRNA before seeding. The knockdown of *Dab1* reduced the effect of Reelin treatment on GRASP65 protein levels ($n = 4$). **B** Neurons were treated for 1 h with 10 µM of either the Src family kinases (SFK) inhibitor PP2 or the vehicle DMSO before and during Reelin treatment. Dab1 was immunoprecipitated from the cell lysate with a rabbit polyclonal antibody against the C-terminal peptide as described in ref. 48. Half of the immunoprecipitated proteins were revealed with a monoclonal anti-Dab1 antibody. The other half of the proteins was revealed using monoclonal anti-phosphotyrosine antibody 4G10 to show the tyrosine phosphorylated Dab1 (P-Dab1). Inhibition of SFK reduced the effect of Reelin on GRASP65 protein level ($n = 4$). $^{**}p < 0.01$, NS not significant.

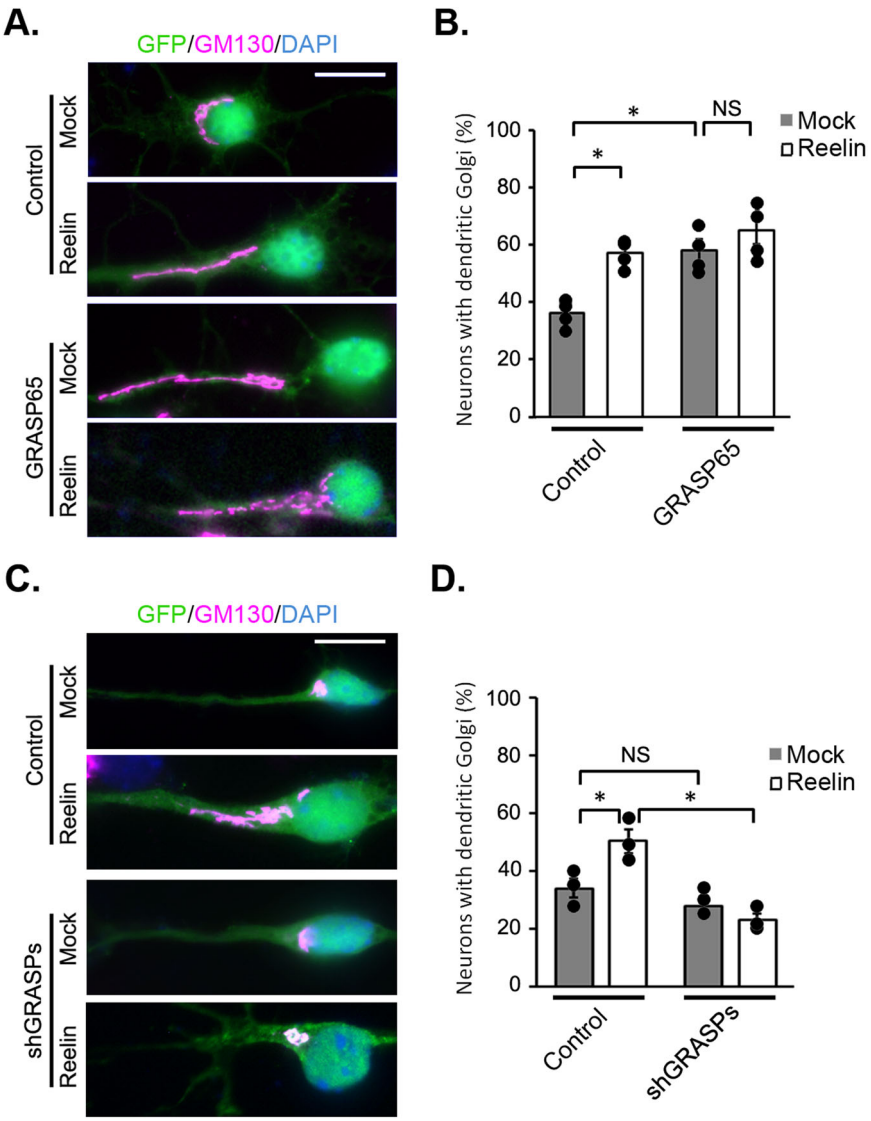

Fig. 3 | GRASPs are key effectors in the Reelin-dependent Golgi translocation into a developing dendrite. Primary cortical neurons were nucleofected with pCAG-GFP along with Control, GRASP65, or shGRASP65 and shGRASP55 expression vectors. After 5 days in culture, neurons were stimulated with Reelin- or Mock- conditioned media for 30 min. Cells were immunostained for GM130, and Golgi location was analyzed in each neuron. **A**, **C** The figure shows examples of neurons with somatic Golgi (Mock) or with dendritic Golgi reaching >8 µm into a dendrite (Reelin or GRASP65). Scale bars: 10 µm. **B, D** The graphs show the percentage of neurons with dendritic Golgi (mean ± s.e.m.). **B** $n = 155$ cells out of 4 experiments for Control + Mock, 157 cells out of 4 experiments for Control + Reelin, 147 cells out of 4 experiments for GRASP65 + Mock, and 152 cells out of 4 experiments for GRASP65 + Reelin. **D** $n = 403$ cells out of 3 experiments for Control + Mock, 325 cells out of 3 experiments for Control + Reelin, 270 cells out of 3 experiments for shGRASPs + Mock, 255 cells out of 3 experiments for shGRASPs + Reelin. $^*p < 0.05$; NS not significant.

knockdown of *Dab1* or by the inhibition of Dab1 tyrosine phosphorylation by SFK (Fig. 2 and Supplementary Fig. S5).

Overall, these results indicate that Reelin and its central active fragment increase GRASPs protein levels in neurons located at the IZ and CP via the stimulation of de novo translation, a function dependent on the canonical Reelin pathway.

GRASPs are key effectors in the Reelin-dependent Golgi deployment and dendritic growth

GRASPs are regulators of Golgi morphology[29], and previous studies have indicated that Reelin plays a role in the morphology and subcellular distribution of the Golgi apparatus[23–26]. To investigate the significance of GRASPs in Reelin-mediated Golgi deployment, primary cortical neurons were nucleofected with either control or GRASP65 expression plasmids. After 5 days in culture, neurons were subsequently stimulated with either Mock- or Reelin-conditioned media. Both Reelin stimulation and the overexpression of GRASP65 resulted in a similar increase in the proportion of neurons exhibiting a Golgi apparatus elongated into a dendrite. Remarkably, the combination of Reelin stimulation and GRASP65 overexpression did not yield an additive effect, implying that they operate within the same signaling pathway (Fig. 3A, B).

Next, two shRNAs were designed to efficiently knockdown GRASP55 and GRASP65 expression, respectively (Supplementary Fig. S6). In order to avoid potential compensatory mechanisms, GRASP65 and 55 were simultaneously downregulated in the following experiments. Primary cortical neurons were nucleofected with either control or the shRNAs targeting GRASPs expression plasmids and placed into culture. 5 days later, neurons were stimulated with either Mock- or Reelin-conditioned media. The knockdown of GRASPs completely abrogated the Golgi deployment induced by Reelin in cultured primary cortical neurons (Fig. 3C, D), further underscoring the importance of GRASPs in this Reelin-induced function.

While Reelin is known to promote dendritic growth in vitro[20–22], the direct involvement of Golgi morphology modulation in this process had not been previously examined. To explore the role of GRASPs in Reelin-stimulated dendritic growth, primary neurons were nucleofected with control or shGRASPs expression plasmids. The next day, cells were incubated for 3 days with Mock- or Reelin-conditioned media. The knockdown of GRASPs efficiently blocked the increase in dendritic growth induced by Reelin (Fig. 4A, B).

Altogether, these results indicate that Reelin induces an increase in GRASPs protein levels to control Golgi remodeling and stimulate dendritic growth.

GRASP65 and GRASP55 knockdowns disturb neuronal migration and layer positioning in vivo

The inhibition of the Reelin pathway leads to defects in neuronal migration and dendrite development in vivo[4,14,17,18,20–22]. The evidence we have gathered so far indicates that GRASPs might be involved in these Reelin-dependent

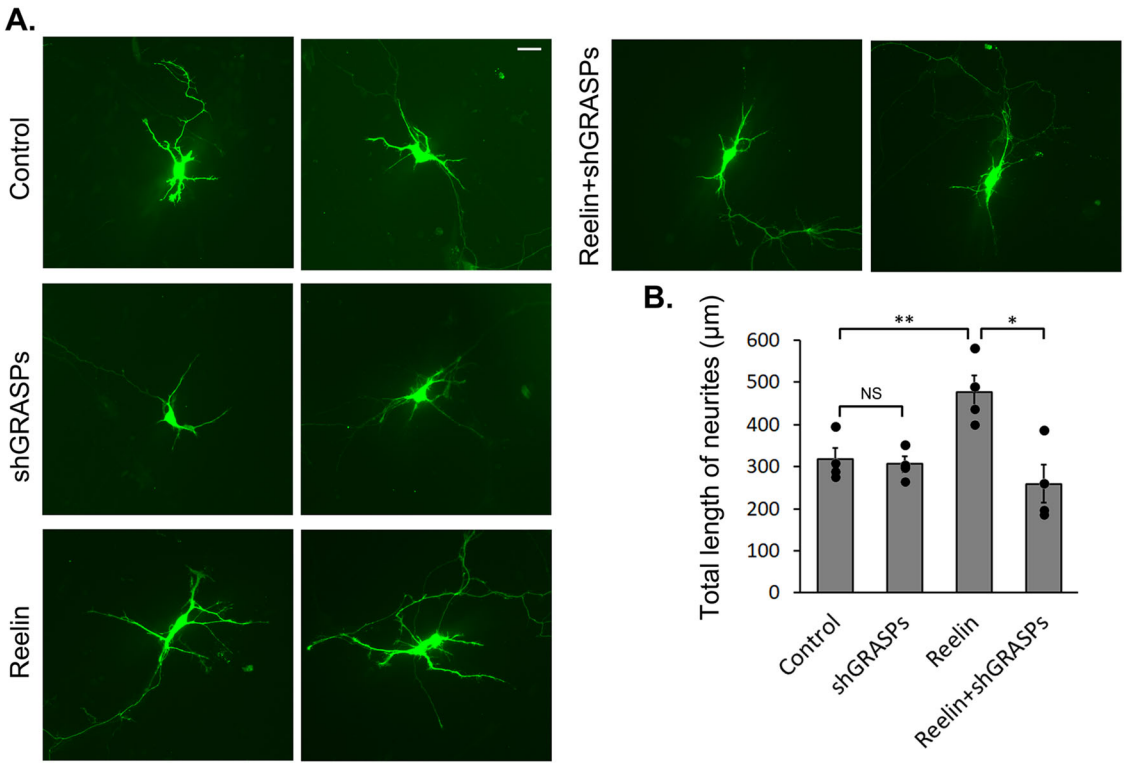

Fig. 4 | GRASPs are key effectors in the Reelin-dependent dendritic growth. Primary cortical neurons were nucleofected with pCAG-GFP along with Control or shGRASP65 and shGRASP55 expression vectors. The next day, neurons were stimulated with Reelin- or Mock- conditioned media for 3 days. **A** The figure shows 2 examples of neurons for each condition. Scale bar: 10 µm. **B** The graph shows the total length of dendrites in µm (mean ± s.e.m.). $n = 173$ cells out of 4 experiments for Control + Mock, 174 cells out of 4 experiments for shGRASPs + Mock, 188 cells out of 4 experiments for Control + Reelin, and 181 cells out of 4 experiments for shGRASPs + Reelin. $^{*}p < 0.05$, $^{**}p < 0.01$, NS not significant.

processes and that the downregulation of GRASPs is likely to cause a comparable phenotype. First, we sought to investigate the role of GRASP proteins in the radial migration of cortical projection neurons. We employed an acute loss-of-function approach using RNA interference combined with in utero electroporation in mice. shRNAs targeting GRASP65 and GRASP55 were co-electroporated with GFP expression plasmids into developing cortices at embryonic day 14.5 (E14.5). Embryos were then processed for histology at E18.5, allowing 4 days of in vivo development. Cerebral walls from histological sections were divided into 10 bins from the apical to the basal sides, and the proportions of GFP^{+} cells were quantified in each bin. In control brains, the majority of electroporated cells were localized to the upper region of the CP. In contrast, a significant number of cells subjected to the simultaneous knockdown of GRASP55 and GRASP65 were stalled in the multipolar migration zone (MMZ) (Fig. 5A). The knockdown of GRASP65 alone resulted in a somewhat smaller yet significant defect, while the shGRASP55 did not perturb migration. However, a higher concentration of shGRASP55 was able to induce a minor but significant position defect of the electroporated cells. Consistent findings were observed with two additional shRNAs targeting different sequences of GRASP65 and GRASP55 (Supplementary Fig. S7).

The examination of brains at postnatal day seven (P7), a stage at which migration of cortical projection neurons is complete, revealed that most of the electroporated neurons successfully reached their final destination at the top of the cerebral wall in control brains. In contrast, while many GRASPs inhibited neurons were able to reach the upper layers, some of them remained dispersed throughout the height of the cerebral wall (Fig. 5B). In addition, the bulk of GRASPs-downregulated cells that reached the top of the CP were positioned further away from the pia when compared to their control counterparts (Fig. 5B).

Cortical neurons generated at E14.5 are primarily destined for the upper layers, with a significant proportion expressing Satb2, which serves as a marker for layer II-IV and callosal projection neurons[54,55]. Our investigation revealed that cells knocked down for GRASPs did not present differentiation defects, as evidenced by their immunopositivity for Satb2 (Fig. 6A). Additional controls showed that downregulation of GRASPs did not affect the $Nestin^{+}$ radial glia fibers, which serve as the migratory substrate for radially migrating neurons, nor did it alter the proportion of $Sox2^{+}$ radial glia cells, of $Tbr2^{+}$ basal progenitors, or the processes of cell proliferation and apoptosis (Fig. 6B–F).

Together, these results show that GRASPs regulate the migration of cortical neurons and their subsequent positioning within the CP.

GRASPs control the orientation of multipolar neurons in vivo

To gain insight into the mechanism underlying the migration defect, we initially analyzed the morphology of migrating neurons within the multipolar migration zone (MMZ) 2 days after electroporation, a period during which the control cells are also mostly in the multipolar phase. We found that the knockdown of GRASPs did not affect the number and length of neurites, nor did it alter the length-to-width ratio of the cell bodies (Fig. 7A–D).

Given that the decrease in GRASP proteins led to the accumulation of cells at the multipolar phase during the embryonic period, and considering that the Reelin pathway has been implicated in the orientation of multipolar migrating neurons[17,18], we proceeded to assess the positioning of the Golgi apparatus specifically in these cells (Fig. 7E, F). Our findings indicated a significant disorientation of MMZ neurons following the knockdown of both GRASP55 and GRASP65, with a substantial reduction of cells exhibiting their Golgi oriented towards the CP. Subsequently, we evaluated the morphology of locomoting neurons in the radial migration zone (RMZ) 4 days after electroporation (Fig. 7G–I). The few GRASPs-inhibited locomoting neurons migrating in the RMZ displayed a longer leading process compared to control cells, while the length-to-width ratio of the cell bodies

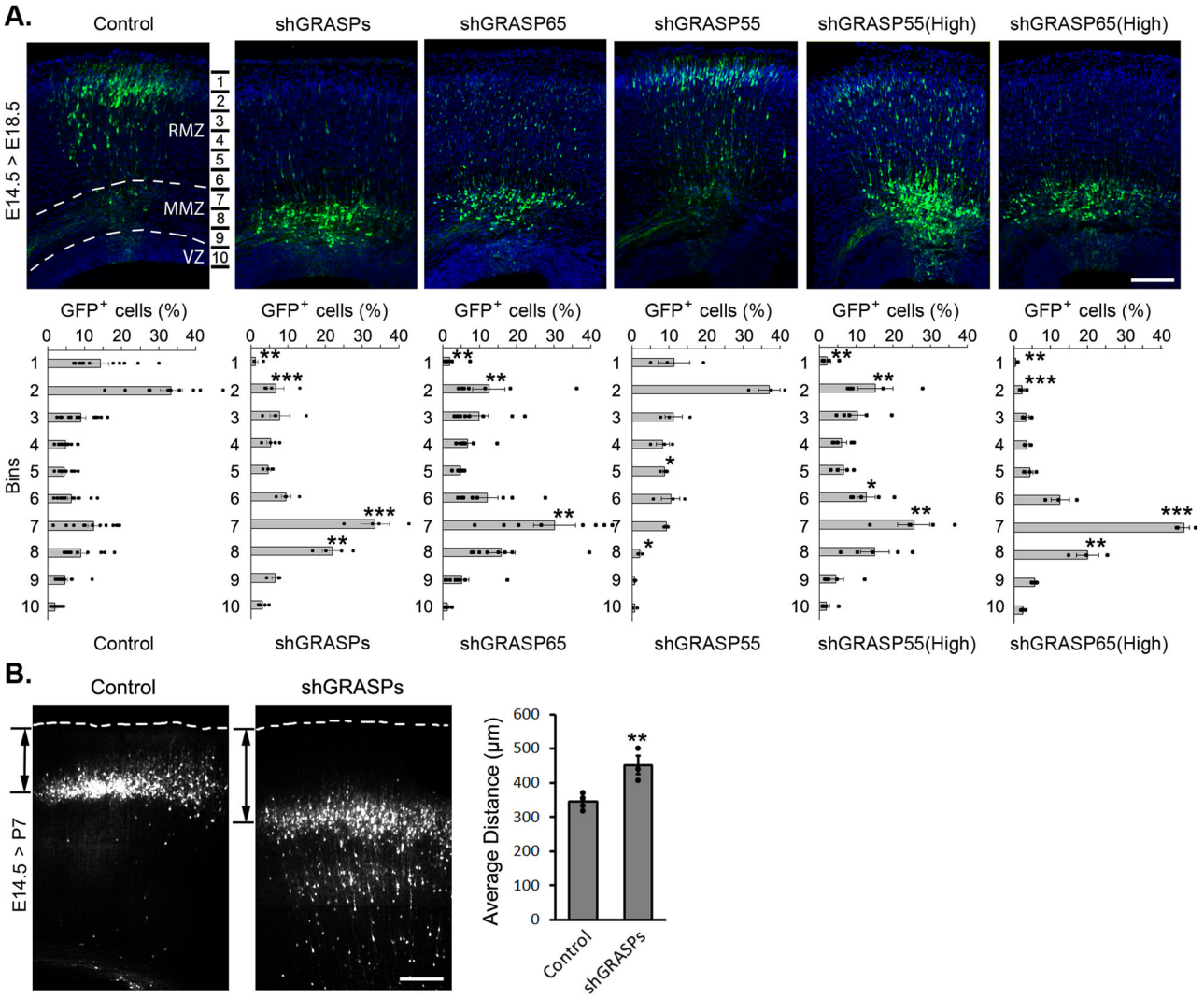

Fig. 5 | GRASPs control neuronal migration and position in vivo. Control or shRNA against *GRASP65*, *GRASP55*, or both (shGRASPs) were co-electroporated in utero with the pCAG-GFP plasmid at embryonic day 14.5 (E14.5). **A** 4 days later at E18.5, cryosections were processed and labeled for DAPI (blue) and GFP (green). The cerebral wall was subdivided into 10 equal bins. Graphs show the percentage of cells in each bin (mean ± s.e.m.). $n = 12$ Control, 4 shGRASPs, 8 shGRASP65, 3 shGRASP55, 5 shGRASP55 (High), 3 shGRASP65 (High). Scale bar 100 µm. VZ: Ventricular zone, MMZ: Multipolar migration zone, RMZ: Radial morphology zone. **B** 12 days later at postnatal day 7 (P7), brains were fixed, cut into 100 µm slices, and processed for microscopy. The average distance between the bulk of electroporated neurons that are located in the upper area, and the cortical surface was measured. The cells that are still migrating in the lower part of the cerebral wall were not included in this measurement. Scale bar 200 µm. The graph shows average distance from the cortical surface (mean ± s.e.m.). $n = 4$ Control, 3 shGRASPs. $^{*}p < 0.05$, $^{**}p < 0.01$, $^{***}p < 0.001$.

remained consistent across both experimental conditions. Although axonal growth was not specifically investigated, we noted the presence of an axon at the rear of locomoting neurons from both control and GRASPs-downregulation conditions (Fig. 7G).

These data indicate that GRASPs play a significant role in guiding the migration of multipolar neurons towards the CP, as evidenced by the mis-positioning of the Golgi apparatus. This defect is likely a contributing factor to the neuronal positioning abnormalities observed in later postnatal stages.

GRASPs control Golgi distribution and dendrite morphogenesis in postnatal brains in vivo

Our findings indicate that GRASPs play a role downstream of Reelin in the regulation of Golgi distribution and dendrite development in vitro. Consequently, we aimed to investigate the function of GRASPs in neocortical dendritogenesis in vivo. In the cerebral cortex, the process of dendrite morphogenesis starts following the completion of neuronal migration. We investigated the consequences of GRASPs knockdown on dendritic development of neurons that were electroporated at E14.5 and analyzed at P7. To assess potential alterations in the morphology of neurons located in layer II/III, we conducted GFP fluorescence-based reconstructions after sparse labeling of electroporated neurons, which allowed the observation of dendrites from distinctly separated cells[56]. As expected, control neurons exhibited a long primary apical dendrite facing perpendicularly the pial surface, a few secondary dendritic branches extending into layer I, and several smaller basal dendrites emanating from the cell body (Fig. 8A, B). In contrast, depletion of GRASP55 and 65 resulted in a shorter apical dendrite (Fig. 8A-C), which extended obliquely towards the pial surface (Fig. 8A, B, D), while the basal dendrites exhibited increased length compared to those in control neurons (Fig. 8A, B, E). These results imply that GRASPs are crucial for the oriented asymmetric growth of dendrites in vivo.

To validate the similarities with the Reelin pathway in dendrite morphogenesis in vivo, we employed a dominant negative form of one of the Reelin receptors, VLDLR (VLDLRΔC), previously used and validated[17]. We further confirm here its ability to inhibit the Reelin-induced Dab1 phosphorylation in primary cortical neurons (Supplementary Fig. S8). The suppression of the Reelin pathway produced a comparable, albeit less

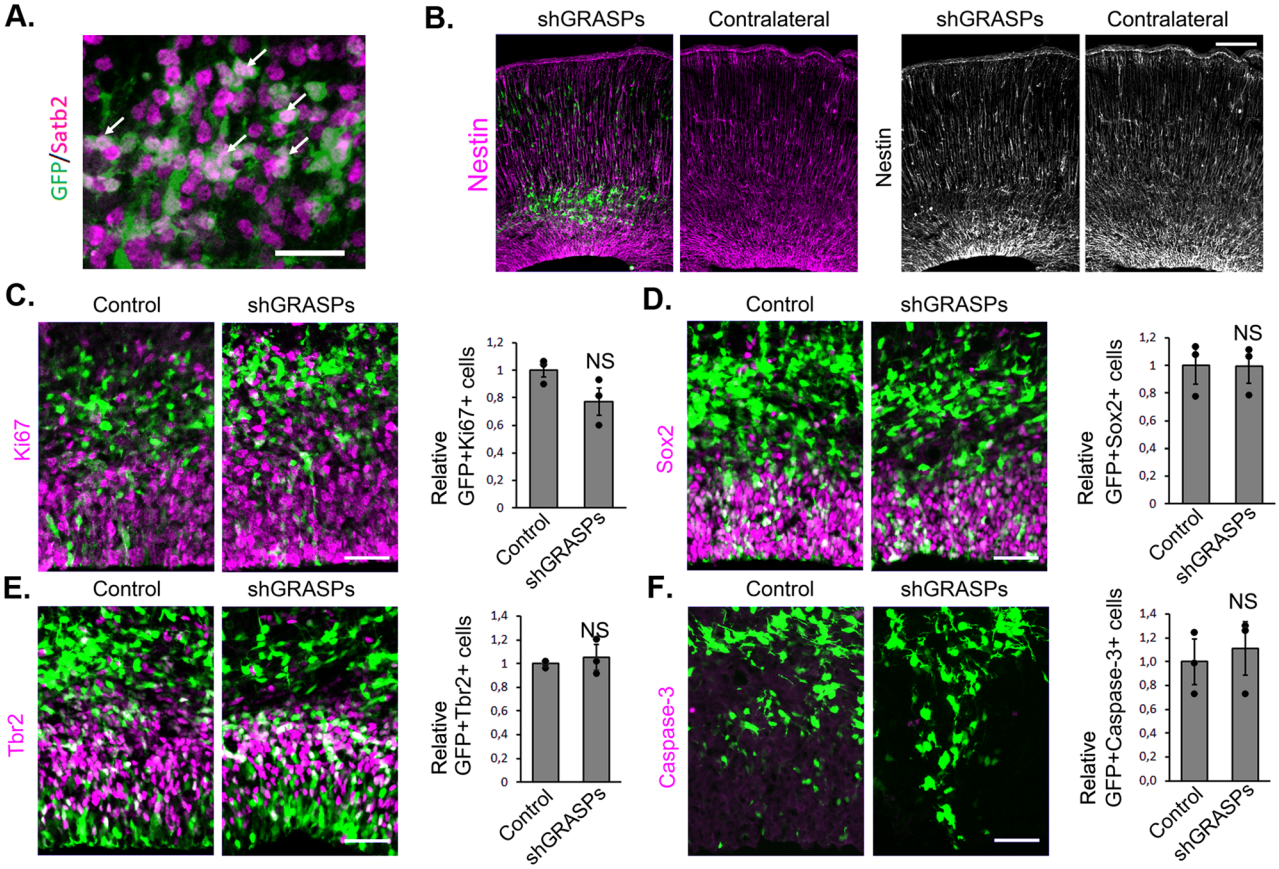

Fig. 6 | GRASPs inhibition does not affect cell fate, radial glia fibers morphology, or proliferation and death of electroporated cells. In utero electroporation for the expression of GFP (Control) or GFP along with shGRASP65 and shGRASP55 was performed at embryonic day E14.5 and analyzed 2 days later. Neurons were labeled for GFP (green) and specific markers (magenta). Inhibition of GRASPs did not affect: **A** neuronal fate. GRASPs-depleted multipolar neurons (green) are positive for Satb2. **B** the radial glia fibers (Nestin), **C** cell division (Ki67), **D** apical (Sox2) or **E** basal (Tbr2) progenitor cells, or **F** cell survival (cleaved Caspase-3). The graphs show the quantification of the number of labeled electroporated cells in a constant area of each section and averaged across sections from at least three different embryos for each antibody. Values are normalized to control (set to 1). (mean ± s.e.m.). $n = 3$ Control and 3 shGRASPs. NS not significant. Scale bars: 100 µm in (**A**) and 50 µm in (**B**–**E**).

pronounced, impact on the growth of apical and basal dendrites in vivo when compared to the knockdown of GRASPs (Fig. 8A–E). We then investigated the positioning and morphology of the Golgi apparatus. Unlike control cells that displayed a polarized Golgi extending from the soma to the apical dendrite, neurons inhibited for GRASPs or for the Reelin pathway exhibited a disorganized Golgi dispersed across multiple dendrites (Fig. 8F). Overall, these findings indicate that inhibitions of GRASPs and of the Reelin pathway lead to similar defects in Golgi distribution, along with faulty dendritogenesis. However, the knockdown of GRASPs manifests a more pronounced phenotype compared to the inhibition of Reelin. Indeed, the silencing of GRASPs by shRNAs likely exerts a stronger effect on its protein levels compared to VLDLR(ΔC) overexpression, which only prevents the upregulation of GRASPs induced by Reelin and does not affect the basal levels of GRASPs proteins.

Discussion

In the majority of cells, the Golgi apparatus plays a crucial role in establishing cellular polarity. As a key element of the secretory pathway, its specific localization within subcellular regions directs secretory activities toward a determined side of the cell. The Golgi's mobility is attributed to the dynamic nature of its structure, which is modulated by various structural proteins, such as GRASP55 and GRASP65, in conjunction with Golgins and other interacting partners[57]. For instance, GRASP65 is essential for orienting the Golgi towards the leading edge in normal rat kidney cells (NRK cells) during migration from a scratch wound[30]. In this study, we investigated the role of GRASPs in the development of the cerebral cortex. The knockdown of one or both GRASPs resulted in impaired migration of projection neurons within the embryonic cerebral wall, causing a delay in their positioning within the CP. This was partly due to the disorientation of the multipolar migration, which was associated with abnormal Golgi positioning and aberrant length of the leading process during locomotion. Postnatally, the downregulation of GRASPs led to an inadequate polarized Golgi morphology and disrupted dendrite morphogenesis, characterized by a shorter misoriented apical dendrite and more developed basal dendrites, along with a shift in the position of the neuronal soma. Additionally, we discovered that the stimulation of neocortical neurons by Reelin enhances the protein levels of GRASPs through de novo translation. This increase is critical for initiating Reelin-dependent morphological alterations in the Golgi apparatus, which are known to influence Golgi functions and promote dendritic growth. The effects of Reelin on Golgi deployment and dendritic growth are both abrogated by the knockdown of GRASPs. Supporting these new findings, the phenotypes we observed in the developing neocortex following GRASPs downregulation closely resemble those resulting from the absence of Reelin signaling as previously documented[4,17,18,23,24,58] and in this study.

Our findings align with previous research indicating that Reelin plays a crucial role in the remodeling of the Golgi apparatus in both cultured neurons and in vivo studies[23–26]. It was proposed that Reelin and the LKB1/Stk25 signaling pathways exert opposing influences on Golgi morphology, albeit through different mechanisms that remain to be elucidated[25]. In this study, we suggest a potential mechanism whereby Reelin promotes Golgi remodeling, at least partially, by enhancing the levels of GRASPs proteins. We further show that Reelin selectively upregulates de novo translation of

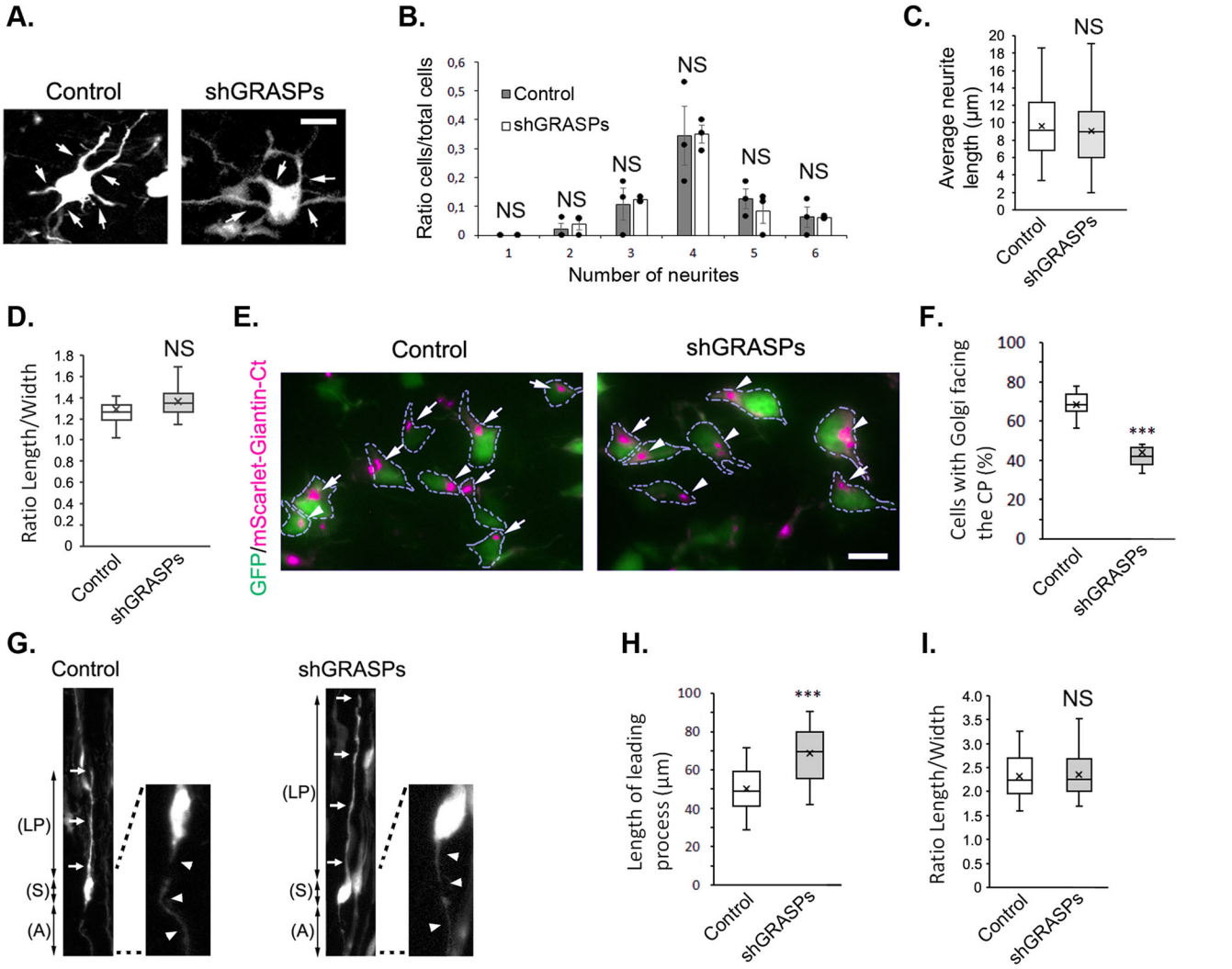

Fig. 7 | GRASPs control multipolar neurons' orientation in vivo. Control or shRNA against *GRASP65* and *GRASP55* were co-electroporated in utero with pCAG-GFP at E14.5. **A**–**F** 2 days or (**G**–**I**) 4 days later, cryosections were processed and labeled for histology. **A**–**E** Inhibition of GRASPs did not alter multipolar neurons development/morphology. **A** High magnification of GFP $^{+}$ multipolar neurons within the MMZ overexpressing control or shGRASPs. Arrows indicate the neurites emanating from neurons. **B** Proportion of GFP $^{+}$ cells with the indicated number of neurites within the MMZ. $n = 129$ neurites out of 31 cells out of 3 control brains, $n = 128$ neurites from 32 cells out of 3 shGRASPs brains. **C** Average multipolar neurons neurite length. $n = 71$ neurites from 19 cells out of 4 control brains, $n = 75$ neurites from 20 cells out of 4 shGRASPs brains. **D** Ratio of length/width of the GFP $^{+}$ cells within the MMZ as an indicator of cell shape. $n = 19$ cells out of 4 control brains, $n = 20$ cells out of 4 shGRASPs brains. **E**, **F** GRASPs-inhibited multipolar neurons are disoriented. **E** The Golgi marker mScarlet-Giantin-Ct (purple) was co-expressed by MMZ neurons (green). The figure shows examples of multipolar neurons with their Golgi facing the CP (white arrows) or facing other directions (white arrowheads). **F** The graph shows the percentage of cells with Golgi oriented towards the cortical plate. $n = 332$ cells out of 13 control brains, $n = 187$ cells out of 9 shGRASPs brains. **G**–**I** Inhibition of GRASPs affected the length of the leading process but not the length-to-width morphology of radially migrating cells. **G** High magnification of GFP $^{+}$ locomoting neurons within the RMZ following overexpression of shRNA control or against GRASPs. Arrows indicate the leading process (LP), arrowheads the axon (A), and (S) is for Soma. **H** Length of the leading process of GFP $^{+}$ locomoting cells within the RMZ. $n = 22$ cells out of 3 control brains, $n = 24$ cells out of 4 shGRASPs brains. **I** Ratio of length/width of the GFP $^{+}$ cells within the RMZ as an indicator of cell shape. $n = 22$ cells out of 3 control brains, $n = 24$ cells out of 4 shGRASPs brains. (mean ± s.e.m.). Scale bars: 40 µm for (**A**), 10 µm for (**B**, **F**); $^{***}p < 0.001$, NS Not significant.

GRASPs while not affecting GM130, another structural Golgi protein. Selective translation depends on several factors such as the joint action of *cis*-acting regulatory elements within the mRNA and *trans*-acting factors such as RNA binding proteins and microRNAs[59,60]. The activity and/or specificity of these regulatory factors can be modified by post-translational modification.

The significance of this increase in GRASPs for the elongation of the Golgi ribbon induced by Reelin warrants consideration. Recent investigations have demonstrated that the formation of Golgi ribbon, rather than merely the stacking of cisternae, is contingent upon GRASPs[41,61]. It is plausible that the formation of the Reelin-induced elongation of the Golgi structure within a single dendrite necessitates elevated GRASPs levels to preserve the connectivity of stacks within the ribbon, thereby facilitating inter-stack exchange and the flow of cargo through the Golgi[29]. This could have implications for protein trafficking, sorting, or glycosylation processes. The type of secretion influenced by Reelin and GRASPs in this context remains to be determined. While classical protein secretion may be implicated, it is also conceivable that GRASPs functions in unconventional protein secretion are involved. Notably, although COPII and COPI transport is not essential for unconventional secretion, the rims of Golgi cisternae may serve as a critical source of membranes or a surface for proteins necessary for unconventional secretion[41,62]. Consequently, loss of rim linking and Golgi ribbon formation following GRASPs depletion would also impact this process.

Our findings indicate that both Reelin stimulation or GRASP65 overexpression lead to a similar deployment of an elongated Golgi ribbon

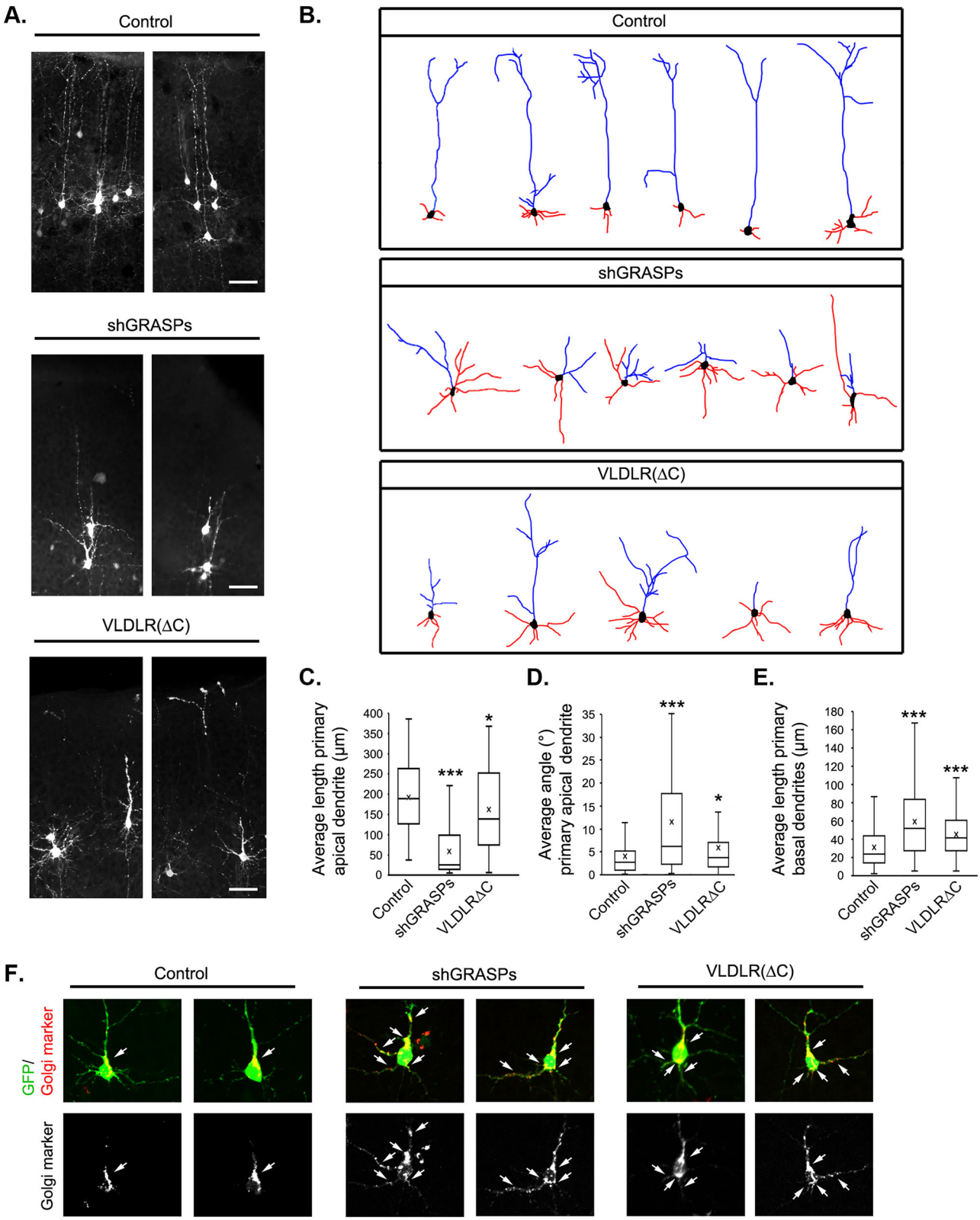

Fig. 8 | GRASPs control Golgi distribution and dendrite morphogenesis in vivo. shRNA against GRASP65 and GRASP55 or a Dominant Negative (DN) VLDLR were co-electroporated in utero with pCAG-GFP and the Golgi marker pCAG-mScarlet-Giantin-Ct at E14.5. 12 days later at P7, brains were fixed and cut into 100 µm-sections to visualize GFP (green) and mScarlet-Giantin-Ct (Red). **A** Representative GFP$^+$ neuron for each condition. Scale bars: 50 µm. **B** Camera lucida drawings of representative neurons displaying the apical (blue) and basal (red) dendrites. **C**–**E** The graphs show (**C**) the average length of the primary apical dendrite. Control $n = 115$ from 4 brains, VLDLR(ΔC) $n = 76$ from 3 brains, and shGRASPs $n = 42$ from 3 brains.; (**D**) Quantification of the angle of the apical dendrite from the soma. This graph depicts the degrees by which the apical dendrites deviate from the expected 90° towards the pial surface. Control $n = 107$ from 4 brains, VLDLR(ΔC) $n = 75$ from 3 brains, and shGRASPs $n = 37$ from 3 brains; (**E**) the average length of the primary basal dendrites. Control $n = 110$ from 4 brains, VLDLR(ΔC) $n = 78$ from 3 brains, and shGRASPs $n = 34$ from 3 brains. (mean ± s.e.m.). $^*p < 0.05$, $^{***}p < 0.001$. **F** Representative GFP$^+$ mScarlet-Giantin-Ct $^+$ neurons for each condition. Arrows show the localization of Golgi structures.

into a single dendrite. Furthermore, downregulation of GRASPs prevents the effect of Reelin on the Golgi apparatus and on dendritic growth. The elongation of the Golgi ribbon into the apical dendrite may play a crucial role in the establishment of Golgi outposts, thereby promoting dendrite growth and branching[11,12]. If this process is disrupted, it could result in the unregulated development of basal dendrites, as observed here when the Reelin pathway or GRASP proteins are inhibited in vivo.

Interestingly, cells destined for layer II/III and knocked down for GRASPs position their soma in the upper layers, albeit at a greater distance from the pial surface compared to control cells. This observation is reminiscent of a defect in the terminal somal translocation, the final phase of cortical pyramidal neuron migration, which is also regulated by Reelin and its downstream effector Rap1[2,4,63]. It is plausible that α5β1 integrin is among the proteins whose secretion is modulated by GRASPs to facilitate terminal translocation[31,63].

The Reelin signaling pathway may not be the sole mechanism capable of regulating GRASPs protein levels in the developing brain. Other pathways may also play a role, either independently or in conjunction with the Reelin pathway. For instance, the Unfolded Protein Response (UPR) has been shown to enhance GRASP55 protein expression in cortical neurons[64]. Interestingly, recent studies suggested noncanonical roles for UPR during the embryonic development of neurons in the central nervous system[65].

Our findings indicate that GRASPs are upregulated by Reelin through de novo translation rather than at the transcriptional level or through inhibition of protein degradation. However, it is important to consider that additional mechanisms, such as phosphorylation, may also influence the regulation of GRASPs activity by Reelin[32,66,67]. Unfortunately, to date, our attempts to utilize specific phospho-GRASP antibodies have not yielded successful results.

Early studies found that, after its secretion, Reelin is processed at two major sites between the second and third Reelin repeats (N-terminal cleavage) and between the sixth and seventh repeats (C-terminal cleavage), producing five fragments (named N-R2, R3-6, R7-8, N-R6 and R3-8) that could be observed using antibodies against N-terminal, central and C-terminal epitopes[14,47,48,68]. The central fragment (R3-6), containing Reelin repeats three to six, is necessary and sufficient to perform some of Reelin's functions, such as the formation of a well-organized embryonic cortical plate (CP)[47,48]. Nevertheless, the two processing sites seem to carry different physiological significances.

The C-terminal processing might be important to allow N-R6 and the central fragment of Reelin to diffuse within the tissue, enabling them to reach and trigger the signal in multipolar neurons[14]. Indeed, immunofluorescent staining using antibodies against different Reelin epitopes revealed that processing fragments containing the N-terminal and/or central epitopes (N-R2, R3-6 and/or N-R6) diffuse from the site of Reelin secretion at the MZ into the CP and the IZ of the embryonic cerebral cortex, while fragments containing the C-terminal epitope (therefore including the full-length Reelin, R3-8 and R7-8) are only localized at the MZ[47]. Later, another study corroborated these results. Using an antibody that recognizes unprocessed Reelin, they show that the full-length protein is only present near the Cajal-Retzius cells, while an antibody against an N-terminal epitope exhibits a staining deeper in the tissue[69]. Therefore, the full-length Reelin could not trigger an increase in GRASPs protein levels and regulate the Golgi in neurons of the IZ. But, we show in this work that R3-6 is also affecting GRASPs protein levels, supporting the ability of Reelin to regulate GRASPs in multipolar neurons at the IZ.

On the other hand, previous studies claimed that the processing of Reelin at the N-terminal site reduces the degree of phosphorylation induced in the intracellular adapter Disabled 1 (Dab1)[70,71]. However, a more recent model suggests that the N-terminal cleavage rather regulates the duration of Reelin signaling but might be dispensable for neuronal migration[69,72].

Overall, our research provides new insights into the relationship between Reelin and the regulation of the Golgi apparatus, as well as polarity events that occur during various stages of brain development, including neuronal migration and dendritogenesis. Future investigations will be essential to further clarify the molecular interactions between the Reelin signaling pathway and GRASPs, to understand the implications of this interaction for Golgi remodeling and protein secretion, and to identify other proteins that Reelin may regulate through GRASPs while elucidating their roles in neocortical development.

Material and methods

Mice

Animal procedures were carried out in accordance with European guidelines and approved by the animal ethics committee of the Université Catholique de Louvain. CD1 mice were bred in standard conditions. The day of vaginal plug was considered as embryonic day 0.5 (E0.5).

In utero electroporation

In utero microinjection and electroporation were performed at E14.5 as essentially described[73]. In brief, timed pregnant CD1-mice were anesthetized, and uterine horns were exposed under sterile conditions. DNA plasmid solutions at 1 μg/ μL were mixed in 10 mM Tris, pH 8.0, with 0.01% Fast Green. DNA solution was injected into the lateral ventricles of the embryos using needles for injection that were pulled from Wiretrol II glass capillaries (Drummond Scientific) and calibrated for 1 μL injections. Forceps-type electrodes (Nepagene) with 5 mm pads were used for electroporation at five 50 ms pulses of 45 V, using ECM830 electroporation system (Harvard Apparatus). The uterine horns were then placed back into the abdominal cavity, and mice were sutured to allow the continuation of a normal development. Brains were collected at E16.5 and E18.5 (neuronal migration studies) or postnatal day (P) 7 (dendrite development studies).

Histology and cytology immunofluorescence

Brains were collected at E16.5, E18.5 (neuronal migration) or P7 (dendrite development), dissected, and successful electroporations were selected by fluorescence visualization. Positive brains were fixed in a 3.7% paraformaldehyde (PFA) in phosphate-buffered saline (PBS) solution at 4 °C for 3 h for embryonic brains, or overnight for postnatal brains. Embryonic brains were cryoprotected in a 30% sucrose/PBS solution overnight at 4 °C, frozen in optimal cutting temperature compound (OCT) previous sectioning with a cryostat at a thickness of 12 μm, and placed on slides. For selected antibodies, sections were antigen retrieved by immersion of the slides in 0.01 M sodium citrate buffer, pH 6.0, at 95 °C for 20 min. Dissociated neurons cultured on a coverslip were fixed for 10 min in 3.7% PFA PBS solution. Sections and coverslips were permeabilized for 15 min in 0.4% Triton X-100/PBS and blocked for 30 min or 1 h with 4% normal goat serum (NGS) in the permeabilization solution. Primary antibodies were diluted in the blocking solution and sections incubated overnight at 4 °C or cells 1 h at room temperature, followed by a three washing steps in 0.4% Triton X-100/PBS. Secondary antibody incubations were 1 h at room temperature in the blocking solution. Nuclei were stained with 4,6-diamidino-2-phenylindole (DAPI), and slides and cells were washed two times with 0.4% Triton X-100/PBS and one time with PBS. Sections and cells were coverslipped with Fluorescence mounting medium (Dako). Images were acquired with a Zeiss AxioVert.A1 fluorescence microscope. Postnatal brains were washed three times for 5 min in PBS, embedded in 4% agar/PBS, and sectioned with a vibratome at 100-μm-thickness. Nuclei were floated-stained with DAPI and sections were then washed three times for 5 min in PBS. Sections were mounted on slides and coverslipped with Mowiol (25% Glycerol, 10% Mowiol 4-88, 0.1 M Tris pH 8.5, and 2.5% Diazobicyclo-octane). Images were acquired with an Olympus FV1000 confocal microscope as 1.5-μm-spaced z-stacks with a 20X objective. Z-sections were stacked using the "Average intensity" method and analyzed with the NeuronJ plugin (E. Meijering 2004) from ImageJ software. The scale used was 1.6103 pixels/μm.

Production of recombinant Reelin, R3-8, and R3-6 fragments

HEK293T cells cultured in standard conditions were transfected with the Reelin, R3-8, or R3-6 cDNA constructs[48] using Polyjet reagent (Tebu-Bio). The day after transfection, medium was replaced for serum-free medium

and collected 2 days later with the addition of an EDTA-free protease inhibitor cocktail (Complete, Roche). The media were stored at 4 °C until use, when it was concentrated with a 100 K Amicon Ultra filtered columns (Millipore) to reach the approximate concentration of 400 pM, as previously described[48]. Concentrated medium was dialyzed for 30 min against neuronal culture medium with plain PTFE Membrane Filters (Millipore). Mock medium was prepared from control transfected HEK293T cells and used to monitor potential co-purifying proteins.

Primary cortical neurons isolation, nucleofection and culture

Neurons were dissected from E14.5 to E17.5 mouse embryo cerebral cortices and seeded on 12-well plate coated with poly-D-lysine and E-C-L (Entactin-Collagen IV-Laminin) Cell Attachment Matrix (Upstate Biotechnology) at a density of 4–6 × 10^6 cell per well. Cells were cultured in Neurobasal medium (Gibco) supplemented with 2% B27 and 1% Penicillin/Streptomycin at 37 °C in a 5% CO_2 incubator. After 3 days in culture, neurons were stimulated with Reelin or Mock-conditioned media. Epoxomicin (Sigma) at 250 nM for 4 h inhibits the proteasome; Leupeptin (Roth) at 0.3 mM for 2 h inhibits the lysosome; Z-VAD-FMK (Selleckchem) at 100 µM for 24 h inhibits Caspase3-dependent cleavage; Anisomycin (Selleckchem) at 40 µM for 45 min inhibits protein translation. DNA plasmid nucleofection was performed with the Amaxa electroporator as described by the manufacturer using the A-033 program and 0.2 mm cuvettes. Cells were resuspended in 100 µL of electroporation buffer plus 3–5 µg of plasmid DNA. Neurons recovery was in Neurobasal medium + 10% of Horse serum (Fisher). For biochemistry, cells were lysed with ice-cold NP-40 buffer (150 mM NaCl, 50 mM Tris-HCl (pH 8.0), 1% NP-40, 5 mM EDTA, and protease and phosphatase inhibitor cocktail (Roche)). For immunofluorescence, cells treated as described above.

Cell lines culture

HEK293T or HeLa cell lines (ATCC) were maintained in Dulbecco's modified Eagle's medium (DMEM) supplemented with 10% FBS, 100 IU/mL penicillin, and 100 mg/mL streptomycin. Cells were cultured in mycoplasma-free conditions at 37 °C under 5% CO_2. Transfection was performed with the PolyJet reagent (Tebu-Bio), following the manufacturer's instructions. Transfected cells were incubated overnight before cell lysis for protein analysis or before fixation for immunofluorescence.

RT-qPCR

Reverse transcription was performed with the iScript cDNA synthesis kit (Biorad), using aliquots of total RNA extracted from neurons obtained with the PureLink RNA Mini Kit (Invitrogen). Quantitative PCR reactions were performed in triplicate using the iTaq Universal SYBR Green Supermix (Bio-Rad) on an iCycler IQ multicolor real-time PCR detection system (Bio-Rad) using the Bio-Rad CFX manager software. Primer sequences (all in 5′–3′ orientation) of target genes and probes are as follows: GAPDH (TGCGACTTCAACAGCAACTC and ATGTAGGCCATGAGGTC CAC); GRASP65 (TGACCTCCACAGCTGTTTCA and CTGGACT GTCTGGGAAGGAG); GRASP55 (CAGCCTCTCCAACTTCAACC and AGGTGCAATGCCAGGTAAGT); Egr1 (GAGCGAACAACCCTATGA GC and GAGTCGTTTGGCTGGGATAA). The relative quantification in gene expression was determined using the 2-ΔΔCt method[74], and GAPDH was used as a reference gene. Using this method, we obtained the fold changes in gene expression normalized to an internal control gene, and relative to one line (calibrator).

Western blot

Proteins were separated by SDS-polyacrylamide gel electrophoresis in Running buffer containing 25 mM Tris Base, 192 mM Glycine, and 0.1% SDS, and then transferred to PVDF membrane (Fisher) in Transfer buffer (25 mM Tris Base, 192 mM Glycine, and 20% methanol) by electroblotting. Transferred membranes were blocked in 5% skimmed milk with 0.05% Tween 20/PBS or in 5% Bovine Serum Albumin (BSA) with 0.05% Tween 20/TBS, both cases for 1 h at room temperature. Antibody incubations were performed in blocking solution, overnight at 4 °C for primary antibody and 1 h at room temperature for secondary antibody conjugated to horseradish peroxidase. Antibody incubations were followed by three washings in PBS or TBS with 0.05% Tween 20. Detection was carried out with the Supersignal West Pico chemiluminescent substrate (Pierce) and exposed to Hyperfilm ECL (Amersham Biosciences).

Antibodies

The following antibodies were used for immunofluorescence: mouse anti-Ki67 (Beckton Dickinson), mouse anti-Sox2 (Cell Signaling), rabbit anti Tbr2 (Abcam), mouse anti-Satb2 (Abcam), rabbit anti-cleaved caspase 3 (Cell Signaling), mouse GM130 (Beckton Dickinson), and Goat secondary antibodies labeled with Alexa 488, 568, and 647 (Invitrogen).

The following antibodies were used for biochemistry: mouse anti-HA.11 clone 16B12 monoclonal antibody (Eurogentec), anti mono- and poly-ubiquitinated antibody clone FK2 (Enzo), mouse anti-β-Actin (Thermo Pierce), anti-phosphotyrosine antibody 4G10 (Upstate Biotechnology), anti-Reelin R4B directed against the central fragment[47], rabbit anti-GFP (Invitrogen), mouse GM130 (Beckton Dickinson), rabbit anti-GRASP55 (Invitrogen), rabbit anti-GRASP65 (Invitrogen), mouse anti-GRASP65 (Santa Cruz), and goat anti-mouse or anti-rabbit horseradish peroxidase-conjugated secondary antibodies (Cell Signaling).

Vector construction

VLDLRΔC, described before[17], contains the extracellular and transmembrane regions and was deleted for part of its cytoplasmic tail (residues 828–873). pmScarlet_Giantin_C1 was a gift from Dorus Gadella (Addgene plasmid # 85048; http://n2t.net/addgene:85048; RRID:Addgene_85048) and inserted into the pCAG vector by PCR using junction primers at the EcoRI and KpnI sites already present in the sequence. GRASP65 and GRASP55 were amplified from E16.5 embryonic mouse cortex and cloned into the pCAG vector with a HA or a GFP tag inserted. Double-stranded oligonucleotides coding for GRASP55 shRNA #1 (target sequence, 5′- GCTATGGTTATTTG CACCGAA -3′), GRASP55 shRNA #2 (target sequence, 5′- CCCTG TCATGACTACTGCAAA -3′), GRASP65 shRNA #1 (target sequence, 5′- CTCTGAAGCTGATGGTGTATA -3′), GRASP65 shRNA #2 (target sequence, 5′- ACCTCACAACTTACTGCCTTT -3′) were cloned downstream of the U6 promoter into the pSilencer2.1-CAG-Venus (pSCV2)-plasmid (a kind gift from F. Polleux, the Scripps Research Institute). Control shRNA (target sequence, 5′- ACTACCGTTGTTATAGGTG -3′) cloned into pSCV2 is a generous gift from P Vanderhaeghen (VIB-KULeuven).

Statistics and reproducibility

In order to avoid bias, picture acquisitions and measurements for neuronal cultures were performed on blinded coverslips. Statistical significance was determined by a Student's t-test for two-population comparisons, or one-way ANOVA followed by Bonferroni's post hoc test for multiple comparisons across N samples, where N is either the number of cells, the number of embryos, or the number of experiments as defined in the figure legends. Data are reported as means ± standard error of the means (s.e.m.), and the statistical significance was set as P value of <0.05.

Reporting summary

Further information on research design is available in the Nature Portfolio Reporting Summary linked to this article.

Data availability

All data supporting the findings of this study are available within the paper and its Supplementary Information. The source data behind the graphs in the paper can be found in Supplementary Data 1.

Received: 30 April 2024; Accepted: 28 March 2025;
Published online: 06 April 2025

References

1. Jossin, Y. Molecular mechanisms of cell polarity in a range of model systems and in migrating neurons. *Mol. Cell Neurosci.* **106**, 103503 (2020).
2. Nadarajah, B., Brunstrom, J. E., Grutzendler, J., Wong, R. O. & Pearlman, A. L. Two modes of radial migration in early development of the cerebral cortex. *Nat. Neurosci.* **4**, 143–150 (2001).
3. Tabata, H. & Nakajima, K. Multipolar migration: the third mode of radial neuronal migration in the developing cerebral cortex. *J. Neurosci.* **23**, 9996–10001 (2003).
4. Sekine, K., Honda, T., Kawauchi, T., Kubo, K. & Nakajima, K. The outermost region of the developing cortical plate is crucial for both the switch of the radial migration mode and the Dab1-dependent "inside-out" lamination in the neocortex. *J. Neurosci.* **31**, 9426–9439 (2011).
5. Shoukimas, G. M. & Hinds, J. W. The development of the cerebral cortex in the embryonic mouse: an electron microscopic serial section analysis. *J. Comp. Neurol.* **179**, 795–830 (1978).
6. Whitford, K. L., Dijkhuizen, P., Polleux, F. & Ghosh, A. Molecular control of cortical dendrite development. *Annu. Rev. Neurosci.* **25**, 127–149 (2002).
7. Ravichandran, Y., Goud, B. & Manneville, J. B. The Golgi apparatus and cell polarity: roles of the cytoskeleton, the Golgi matrix, and Golgi membranes. *Curr. Opin. Cell Biol.* **62**, 104–113 (2020).
8. Kon, E., Cossard, A. & Jossin, Y. Neuronal polarity in the embryonic mammalian cerebral cortex. *Front. Cell Neurosci.* **11**, 163 (2017).
9. de Anda, F. C., Meletis, K., Ge, X., Rei, D. & Tsai, L. H. Centrosome motility is essential for initial axon formation in the neocortex. *J. Neurosci.* **30**, 10391–10406 (2010).
10. Hatanaka, Y. & Yamauchi, K. Excitatory cortical neurons with multipolar shape establish neuronal polarity by forming a tangentially oriented axon in the intermediate zone. *Cereb. Cortex* **23**, 105–113 (2013).
11. Horton, A. C. et al. Polarized secretory trafficking directs cargo for asymmetric dendrite growth and morphogenesis. *Neuron* **48**, 757–771 (2005).
12. Ye, B. et al. Growing dendrites and axons differ in their reliance on the secretory pathway. *Cell* **130**, 717–729 (2007).
13. Koenig, M., Dobyns, W. B. & Di Donato, N. Lissencephaly: Update on diagnostics and clinical management. *Eur. J. Paediatr. Neurol.* **35**, 147–152 (2021).
14. Jossin, Y. Reelin functions, mechanisms of action and signaling pathways during brain development and maturation. *Biomolecules* **10**, 964 (2020).
15. Copf, T. Impairments in dendrite morphogenesis as etiology for neurodevelopmental disorders and implications for therapeutic treatments. *Neurosci. Biobehav. Rev.* **68**, 946–978 (2016).
16. Francis, F. & Cappello, S. Neuronal migration and disorders—an update. *Curr. Opin. Neurobiol.* **66**, 57–68 (2021).
17. Jossin, Y. & Cooper, J. A. Reelin, Rap1 and N-cadherin orient the migration of multipolar neurons in the developing neocortex. *Nat. Neurosci.* **14**, 697–703 (2011).
18. Kon, E. et al. N-cadherin-regulated FGFR ubiquitination and degradation control mammalian neocortical projection neuron migration. *Elife* **8**, e47673 (2019).
19. Olson, E. C., Kim, S. & Walsh, C. A. Impaired neuronal positioning and dendritogenesis in the neocortex after cell-autonomous Dab1 suppression. *J. Neurosci.* **26**, 1767–1775 (2006).
20. Jossin, Y. & Goffinet, A. M. Reelin signals through phosphatidylinositol 3-kinase and Akt to control cortical development and through mTor to regulate dendritic growth. *Mol. Cell Biol.* **27**, 7113–7124 (2007).
21. Niu, S., Renfro, A., Quattrocchi, C. C., Sheldon, M. & D'Arcangelo, G. Reelin promotes hippocampal dendrite development through the VLDLR/ApoER2-Dab1 pathway. *Neuron* **41**, 71–84 (2004).
22. Matsuki, T., Pramatarova, A. & Howell, B. W. Reduction of Crk and CrkL expression blocks reelin-induced dendritogenesis. *J. Cell Sci.* **121**, 1869–1875 (2008).
23. Nichols, A. J. & Olson, E. C. Reelin promotes neuronal orientation and dendritogenesis during preplate splitting. *Cereb. Cortex* **20**, 2213–2223 (2010).
24. O'Dell, R. S. et al. Layer 6 cortical neurons require Reelin-Dab1 signaling for cellular orientation, Golgi deployment, and directed neurite growth into the marginal zone. *Neural Dev.* **7**, 25 (2012).
25. Matsuki, T. et al. Reelin and stk25 have opposing roles in neuronal polarization and dendritic Golgi deployment. *Cell* **143**, 826–836 (2010).
26. Meseke, M., Rosenberger, G. & Forster, E. Reelin and the Cdc42/Rac1 guanine nucleotide exchange factor alphaPIX/Arhgef6 promote dendritic Golgi translocation in hippocampal neurons. *Eur. J. Neurosci.* **37**, 1404–1412 (2013).
27. Zhang, X. & Wang, Y. Nonredundant roles of GRASP55 and GRASP65 in the Golgi apparatus and beyond. *Trends Biochem Sci.* **45**, 1065–1079 (2020).
28. Bekier, M. E. et al. Knockout of the Golgi stacking proteins GRASP55 and GRASP65 impairs Golgi structure and function. *Mol. Biol. Cell* **28**, 2833–2842 (2017).
29. Burd, C. G. GRASPing for consensus about the Golgi apparatus. *J. Cell Biol.* **220**, e202103117 (2021).
30. Bisel, B. et al. ERK regulates Golgi and centrosome orientation towards the leading edge through GRASP65. *J. Cell Biol.* **182**, 837–843 (2008).
31. Ahat, E., Xiang, Y., Zhang, X., Bekier, M. E. 2nd & Wang, Y. GRASP depletion-mediated Golgi destruction decreases cell adhesion and migration via the reduction of alpha5beta1 integrin. *Mol. Biol. Cell* **30**, 766–777 (2019).
32. Yoshimura, S. et al. Convergence of cell cycle regulation and growth factor signals on GRASP65. *J. Biol. Chem.* **280**, 23048–23056 (2005).
33. Kinseth, M. A. et al. The Golgi-associated protein GRASP is required for unconventional protein secretion during development. *Cell* **130**, 524–534 (2007).
34. Nuchel, J. et al. An mTORC1-GRASP55 signaling axis controls unconventional secretion to reshape the extracellular proteome upon stress. *Mol. Cell* **81**, 3275–3293.e3212 (2021).
35. Gee, H. Y., Noh, S. H., Tang, B. L., Kim, K. H. & Lee, M. G. Rescue of DeltaF508-CFTR trafficking via a GRASP-dependent unconventional secretion pathway. *Cell* **146**, 746–760 (2011).
36. Kim, J. et al. Monomerization and ER relocalization of GRASP Is a requisite for unconventional secretion of CFTR. *Traffic* **17**, 733–753 (2016).
37. Xiang, Y. et al. Regulation of protein glycosylation and sorting by the Golgi matrix proteins GRASP55/65. *Nat. Commun.* **4**, 1659 (2013).
38. Schotman, H., Karhinen, L. & Rabouille, C. dGRASP-mediated noncanonical integrin secretion is required for Drosophila epithelial remodeling. *Dev. Cell* **14**, 171–182 (2008).
39. Veenendaal, T. et al. GRASP65 controls the cis Golgi integrity in vivo. *Biol. Open* **3**, 431–443 (2014).
40. Chiritoiu, M., Brouwers, N., Turacchio, G., Pirozzi, M. & Malhotra, V. GRASP55 and UPR control interleukin-1beta aggregation and secretion. *Dev. Cell* **49**, 145–155.e144 (2019).
41. Grond, R. et al. The function of GORASPs in Golgi apparatus organization in vivo. *J. Cell Biol.* **219**, e202004191 (2020).
42. Need, A. C. et al. A genome-wide study of common SNPs and CNVs in cognitive performance in the CANTAB. *Hum. Mol. Genet* **18**, 4650–4661 (2009).
43. Rasika, S., Passemard, S., Verloes, A., Gressens, P. & El Ghouzzi, V. Golgipathies in neurodevelopment: a new view of old defects. *Dev. Neurosci.* **40**, 396–416 (2018).

44. Al-Sarraj, Y. et al. Family-based genome-wide association study of autism spectrum disorder in Middle Eastern families. *Genes***12**, 761 (2021).
45. Simo, S. et al. Reelin induces the detachment of postnatal subventricular zone cells and the expression of the Egr-1 through Erk1/2 activation. *Cereb. Cortex* **17**, 294–303 (2007).
46. Lane, J. D. et al. Caspase-mediated cleavage of the stacking protein GRASP65 is required for Golgi fragmentation during apoptosis. *J. Cell Biol.* **156**, 495–509 (2002).
47. Jossin, Y., Gui, L. & Goffinet, A. M. Processing of Reelin by embryonic neurons is important for function in tissue but not in dissociated cultured neurons. *J. Neurosci.* **27**, 4243–4252 (2007).
48. Jossin, Y. et al. The central fragment of Reelin, generated by proteolytic processing in vivo, is critical to its function during cortical plate development. *J. Neurosci.* **24**, 514–521 (2004).
49. Preisinger, C. et al. YSK1 is activated by the Golgi matrix protein GM130 and plays a role in cell migration through its substrate 14-3-3z. *eta. J. Cell Biol.* **164**, 1009–1020 (2004).
50. Puthenveedu, M. A., Bachert, C., Puri, S., Lanni, F. & Linstedt, A. D. GM130 and GRASP65-dependent lateral cisternal fusion allows uniform Golgi-enzyme distribution. *Nat. Cell Biol.* **8**, 238–248 (2006).
51. Kuo, G., Arnaud, L., Kronstad-O'Brien, P. & Cooper, J. A. Absence of Fyn and Src causes a reeler-like phenotype. *J. Neurosci.* **25**, 8578–8586 (2005).
52. Jossin, Y., Ogawa, M., Metin, C., Tissir, F. & Goffinet, A. M. Inhibition of SRC family kinases and non-classical protein kinases C induce a reeler-like malformation of cortical plate development. *J. Neurosci.* **23**, 9953–9959 (2003).
53. Rice, D. S. et al. Disabled-1 acts downstream of Reelin in a signaling pathway that controls laminar organization in the mammalian brain. *Development* **125**, 3719–3729 (1998).
54. Alcamo, E. A. et al. Satb2 regulates callosal projection neuron identity in the developing cerebral cortex. *Neuron* **57**, 364–377 (2008).
55. Britanova, O. et al. Satb2 is a postmitotic determinant for upper-layer neuron specification in the neocortex. *Neuron* **57**, 378–392 (2008).
56. Luo, W. et al. Supernova: a versatile vector system for single-cell labeling and gene function studies in vivo. *Sci. Rep.* **6**, 35747 (2016).
57. Petrosyan, A. Unlocking golgi: why does morphology matter?. *Biochem. (Mosc.* **84**, 1490–1501 (2019).
58. O'Dell, R. S., Cameron, D. A., Zipfel, W. R. & Olson, E. C. Reelin prevents apical neurite retraction during terminal translocation and dendrite initiation. *J. Neurosci.* **35**, 10659–10674 (2015).
59. Tidu, A. & Martin, F. The interplay between cis- and trans-acting factors drives selective mRNA translation initiation in eukaryotes. *Biochimie* **217**, 20–30 (2024).
60. Cagnetta, R., Flanagan, J. G. & Sonenberg, N. Control of selective mRNA translation in neuronal subcellular compartments in health and disease. *J. Neurosci.* **43**, 7247–7263 (2023).
61. Zhang, Y. & Seemann, J. Rapid degradation of GRASP55 and GRASP65 reveals their immediate impact on the Golgi structure. *J. Cell Biol.* **220**, e202007052 (2021).
62. Rabouille, C. Pathways of unconventional protein secretion. *Trends Cell Biol.* **27**, 230–240 (2017).
63. Sekine, K. et al. Reelin controls neuronal positioning by promoting cell-matrix adhesion via inside-out activation of integrin alpha5beta1. *Neuron* **76**, 353–369 (2012).
64. van Ziel, A. M., Largo-Barrientos, P., Wolzak, K., Verhage, M. & Scheper, W. Unconventional secretion factor GRASP55 is increased by pharmacological unfolded protein response inducers in neurons. *Sci. Rep.* **9**, 1567 (2019).
65. Godin, J. D., Creppe, C., Laguesse, S. & Nguyen, L. Emerging roles for the unfolded protein response in the developing nervous system. *Trends Neurosci.* **39**, 394–404 (2016).
66. Jesch, S. A., Lewis, T. S., Ahn, N. G. & Linstedt, A. D. Mitotic phosphorylation of Golgi reassembly stacking protein 55 by mitogen-activated protein kinase ERK2. *Mol. Biol. Cell* **12**, 1811–1817 (2001).
67. Cervigni, R. I. et al. JNK2 controls fragmentation of the Golgi complex and the G2/M transition through phosphorylation of GRASP65. *J. Cell Sci.* **128**, 2249–2260 (2015).
68. Lambert de Rouvroit, C. et al. Reelin, the extracellular matrix protein deficient in reeler mutant mice, is processed by a metalloproteinase. *Exp. Neurol.* **156**, 214–217 (1999).
69. Koie, M. et al. Cleavage within Reelin repeat 3 regulates the duration and range of the signaling activity of Reelin protein. *J. Biol. Chem.* **289**, 12922–12930 (2014).
70. Kubo, K., Mikoshiba, K. & Nakajima, K. Secreted Reelin molecules form homodimers. *Neurosci. Res.* **43**, 381–388 (2002).
71. Kohno, S. et al. Mechanism and significance of specific proteolytic cleavage of Reelin. *Biochem. Biophys. Res. Commun.* **380**, 93–97 (2009).
72. Okugawa, E. et al. Physiological significance of proteolytic processing of Reelin revealed by cleavage-resistant Reelin knock-in mice. *Sci. Rep.* **10**, 4471 (2020).
73. Tabata, H. & Nakajima, K. Efficient in utero gene transfer system to the developing mouse brain using electroporation: visualization of neuronal migration in the developing cortex. *Neuroscience* **103**, 865–872 (2001).
74. Livak, K. J. & Schmittgen, T. D. Analysis of relative gene expression data using real-time quantitative PCR and the 2(-Delta Delta C(T)) Method. *Methods* **25**, 402–408 (2001).

Acknowledgements

This work was supported by grants J.0179.16, T.0243.18, and J.0101.21 from the Belgian National Funding for Scientific Research (FNRS). Y.J. is an FNRS investigator. E.C.J. and K.S. were supported by « Fonds pour la Formation à la Recherche dans l'Industrie et dans l'Agriculture » (FRIA) fellowships.

Author contributions

Y.J. conceived the project. E.C.J., K.S., A.J., and Y.J. performed all experiments and data analysis. Y.J. and E.C.J. wrote the paper.

Competing interests

The authors declare no competing interests.

Additional information

Supplementary information The online version contains supplementary material available at https://doi.org/10.1038/s42003-025-08014-x.

Correspondence and requests for materials should be addressed to Yves Jossin.

Peer review information *Communications Biology* thanks Sergi Simo, Laurent Calvier, and the other anonymous reviewer(s) for their contribution to the peer review of this work. Primary Handling Editors: Alex Nord and Benjamin Bessieres. A peer review file is available.